

ORIGINAL RESEARCH ARTICLE

Mesoscale computational prediction of lightweight, thermally conductive polymer nanocomposites containing graphene-wrapped hollow particle fillers

Jianjun Wang^{1,a,*}, Zhonghui Shen^{2,a}, Wenying Zhou^{3*}, Yang Shen², Cewen Nan², Qing Wang¹, Longqing Chen^{1*}

¹ Department of Materials Science and Engineering, The Pennsylvania State University, University Park, Pennsylvania 16802, United States. E-mail: wjj8384@gmail.com (J Wang); lqc3@psu.edu (L Chen)

² School of Materials Science and Engineering, State Key Lab of New Ceramics and Fine Processing, Tsinghua University, Beijing 100084, China

³ College of Chemistry and Chemical Engineering, Xi'an University of Science & Technology, Xi'an 710054, China. E-mail: wyzhou2004@163.com (W Zhou)

ABSTRACT

Heat removal has become an increasingly crucial issue for microelectronic chips due to increasingly high speed and high performance. One solution is to increase the thermal conductivity of the corresponding dielectrics. However, traditional approach to adding solid heat conductive nanoparticles to polymer dielectrics led to a significant weight increase. Here we propose a dielectric polymer filled with heat conductive hollow nanoparticles to mitigate the weight gain. Our mesoscale simulation of heat conduction through this dielectric polymer composite microstructure using the phase-field spectral iterative perturbation method demonstrates the simultaneous achievement of enhanced effective thermal conductivity and the low density. It is shown that additional heat conductivity enhancement can be achieved by wrapping the hollow nanoparticles with graphene layers. The underlying mesoscale mechanism of such a microstructure design and the quantitative effect of interfacial thermal resistance will be discussed. This work is expected to stimulate future efforts to develop light-weight thermal conductive polymer nanocomposites.

Keywords: Thermal Conductivity; Polymer Nanocomposites; Materials Design; Graphene-Wrapped Hollow Nanoparticles

ARTICLE INFO

Received: 2 February 2021
Accepted: 17 March 2021
Available online: 25 March 2021

COPYRIGHT

Copyright © 2021 Jianjun Wang, *et al.*
EnPress Publisher LLC. This work is licensed under the Creative Commons Attribution-NonCommercial 4.0 International License (CC BY-NC 4.0).
<https://creativecommons.org/licenses/by-nc/4.0/>

1. Introduction

The effective thermal management in applications, such as LED (light emitting diode) lighting, batteries, automobile cooling systems, and high-power density microelectronic devices, where heat accumulation can have deleterious effects, is critically important to ensure the device performance and reliability, and therefore to enhance the lifetime and accuracy of the system^[1-3]. With further miniaturization, integration and functionalization of microelectronics and the emerging applications, such as electronic assembly and packaging, and solar the thermal dissipation has become a challenge^[4-6]. Addressing this challenge requires the development of novel materials with enhanced thermal conductivity as well as light weight, low cost, good processability, and corrosion resistance. Polymers have many of these charac-

^a These authors contributed equally to this work.

teristics, but they generally have very low thermal conductivity ($0.1\text{--}0.4\text{ Wm}^{-1}\cdot\text{K}^{-1}$)^[7,8]. Therefore, heat conductive fillers, such as carbon nanotube^[9–13] ($> 2,000\text{ Wm}^{-1}\cdot\text{K}^{-1}$), graphene^[14–18] ($\sim 5,000\text{ Wm}^{-1}\cdot\text{K}^{-1}$), aluminum oxide^[19–21] ($> 20\text{ Wm}^{-1}\cdot\text{K}^{-1}$), boron nitride^[22–26] ($\sim 350\text{ Wm}^{-1}\cdot\text{K}^{-1}$), and metal particles^[27–31] ($> 100\text{ Wm}^{-1}\cdot\text{K}^{-1}$), etc., are traditionally added into polymers to enhance their thermal conductivity while preserving the above-mentioned advantages of polymers.

The influences of the filler type, size, shape, alignment, and loading level on the effective thermal conductivity of the resulted polymer composites have been extensively investigated, see e.g., the recent reviews^[5,12,32]. It was generally accepted that a high filler loading level ($\geq 30\%$ in volume) is necessary in order to achieve the appropriate level ($\geq 1\text{ Wm}^{-1}\cdot\text{K}^{-1}$) of thermal conductivity in a polymer nanocomposite. For example, heat sinks in micro-electronic systems require polymer nanocomposites with a thermal conductivity approximately from 1 to $30\text{ Wm}^{-1}\cdot\text{K}^{-1}$, which normally needs a filler loading level higher than 30% in volume^[7,33]. The high loading level of the filler, particularly for metallic fillers, usually significantly increases the mass density and costs, and weakens the mechanical performances, such as tensile strength and flexibility, and processibility, which prevents the polymer composites from being used commercially, in particular in aerospace where a lightweight is extremely desired^[32,34]. Therefore, it is imperative to seek for alternative approach-

es to developing novel material microstructures with enhanced thermal conductivity but low density and costs.

To effectively reduce the weight and improve the specific thermal conductivity of filled polymers, in this work, we propose to fill the polymer matrix with hollow nanoparticles to increase the thermal conductivity while preserving a low mass density of the nanocomposite. In particular, we computed the effective thermal conductivity (κ_{eff}) and the effective mass density (ρ_{eff}) of the polyethylene (PE) polymer nanocomposites filled with various hollow nanoparticles. It is predicted that by wrapping a thin graphene layer onto the hollow nanoparticles, the effective thermal conductivity can be further significantly enhanced.

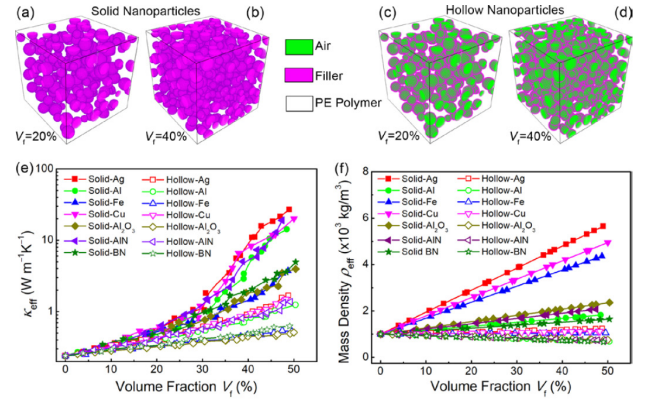


Figure 1. Computationally-generated microstructures for polymer nanocomposites filled with (a) 20 vol.% solid nanoparticles, (b) 40 vol.% solid nanoparticles, (c) 20 vol.% hollow nanoparticles, and (d) 40 vol.% hollow nanoparticles, (e) the effective thermal conductivity and (f) mass density as function of filler volume fraction for polymer nanocomposites filled with various solid and hollow nanoparticles.

Table 1. Thermal conductivities and mass density of the filler materials used in the simulation. For BN nanoparticles, the thermal conductivity used is smaller than the literature values which were reported for the in-plane thermal conductivity in BN nanosheets. For PE polymer, the thermal conductivity depends on the density

Materials	Thermal Conductivity ($\text{Wm}^{-1}\cdot\text{K}^{-1}$)	Mass Density (kg/m^3)	Literature Values ($\text{Wm}^{-1}\cdot\text{K}^{-1}$)	Refs.
Ag	417	10,490	427	31
Al	237	2,700	247	28
Fe	40	7,900	67	38
Cu	397	8,900	398	28
Al_2O_3	33	3,700	30–36	39
AlN	300	3,260	100–300	5
BN	57	2,290	185–300	5,40
Graphene	4,000	2,250	2,000–6,000	41,42
PE polymer	0.24	1,000	0.3–0.45	5
Air	0.024	1.225	0.024	5

2. Methods

The heat conduction equation in the polymer nanocomposite can be written as:

$$\frac{\partial}{\partial x_i} \left(k_{ij}(\mathbf{x}) \frac{\partial T(\mathbf{x})}{\partial x_j} \right) + q(\mathbf{x}) = \rho(\mathbf{x}) c_p(\mathbf{x}) \frac{\partial T(\mathbf{x})}{\partial t} \quad (1)$$

where $k_{ij}(\mathbf{x})$, $T(\mathbf{x})$, $\rho(\mathbf{x})$, and $c_p(\mathbf{x})$ represent the spatial-dependent thermal conductivity tensor, temperature, the mass density, and the specific heat capacity, respectively. Those spatial-dependent material properties such as $k_{ij}(\mathbf{x})$, $\rho(\mathbf{x})$, and $c_p(\mathbf{x})$ are determined by the microstructure of the polymer nanocomposite specified by a phase-field variable. The internal heat source of the material is represented by $q(\mathbf{x})$. Eq. (1) can be solved using the spectral iterative perturbation method which was developed in previous work^[35] or using the finite element method via the COMSOL software. When incorporating the interfacial thermal resistance, slit boundary conditions are applied at the heterointerfaces between phase A and phase B, i.e.,

$$-\mathbf{n}_A \cdot (-\mathbf{k}^A \nabla T_A) = \frac{T_B - T_A}{R_k}, \quad -\mathbf{n}_B \cdot (-\mathbf{k}^B \nabla T_B) = \frac{T_A - T_B}{R_k} \quad (2)$$

where n_A and n_B represent the normal directions of the interface pointing to phase A and phase B, respectively. The variable T_A and T_B represent the temperature at the two boundaries of the heterointerfaces, and k_A and k_B represent the thermal conductivity of phase A and phase B, respectively. Once the temperature distribution is solved, the heat flux density that flows through a unit area per unit time can be determined from the Fourier's law, i.e.,

$$J_i = -k_{ij}(\mathbf{x}) \partial T(\mathbf{x}) / \partial x_j \quad (3)$$

The effective thermal conductivity tensor k_{ij}^{eff} of the polymer nanocomposite can then be determined from Eq. (3) by solving

$$\langle J_i \rangle = -k_{ij}^{\text{eff}} \langle \partial T(\mathbf{x}) / \partial x_j \rangle \quad (4)$$

where $\langle \rangle$ represents the average property per volume.

2. Results and discussions

Figures 1a-d show the microstructures of PE nanocomposites filled with 20 vol.% and 40 vol.%

solid nanoparticles, 20 vol.% and 40 vol.% hollow nanoparticles, respectively, computationally generated assuming random distributions of the filler nanoparticles. For hollow nanoparticles, the thickness of the filler layer is about 4% to 7% of the radius of the nanoparticles. The effective thermal conductivity for the polymer nanocomposite is calculated by solving the steady-state heat conduction equation using the phase-field spectral iterative perturbation method^[35-37]. The intrinsic thermal conductivities and mass densities of the filler materials, polyethylene (PE) polymer, and air used in the computation are listed in **Table 1**.

Figure 1e shows the effective thermal conductivity as function of the filler volume fraction for PE nanocomposites filled with various nanoparticles. For all listed nanocomposites, the effective thermal conductivity increases with the volume fraction of the fillers for both the solid and hollow nanoparticles. For a filler material at a given V_f , the solid nanoparticles are more effective than the hollow nanoparticles in enhancing the thermal conductivity. For example, at a V_f of ~50%, the polymer nanocomposites filled with solid Ag, solid Al, solid Fe, solid Cu, solid Al_2O_3 , solid AlN, and solid BN nanoparticles have a κ_{eff} of ~28 $\text{Wm}^{-1}\cdot\text{K}^{-1}$, ~14 $\text{Wm}^{-1}\cdot\text{K}^{-1}$, ~3.6 $\text{Wm}^{-1}\cdot\text{K}^{-1}$, ~20 $\text{Wm}^{-1}\cdot\text{K}^{-1}$, ~4.1 $\text{Wm}^{-1}\cdot\text{K}^{-1}$, ~22 $\text{Wm}^{-1}\cdot\text{K}^{-1}$, and ~5.0 $\text{Wm}^{-1}\cdot\text{K}^{-1}$, while their counterparts filled with corresponding hollow nanoparticles have a κ_{eff} of ~1.9 $\text{Wm}^{-1}\cdot\text{K}^{-1}$, ~1.2 $\text{Wm}^{-1}\cdot\text{K}^{-1}$, ~0.5 $\text{Wm}^{-1}\cdot\text{K}^{-1}$, ~1.7 $\text{Wm}^{-1}\cdot\text{K}^{-1}$, ~0.5 $\text{Wm}^{-1}\cdot\text{K}^{-1}$, ~1.4 $\text{Wm}^{-1}\cdot\text{K}^{-1}$, and ~0.6 $\text{Wm}^{-1}\cdot\text{K}^{-1}$, respectively (see **Table 2**).

However, the effective mass density of the PE nanocomposite is significantly increased by the solid nanoparticles compared to the hollow nanoparticles. As shown in **Figure 1f**, at a V_f of ~50%, the nanocomposites filled with solid Ag, solid Cu, and solid Fe nanoparticles respectively have a ρ_{eff} of ~5,646 kg/m^3 , ~4,971 kg/m^3 , and ~4,374 kg/m^3 , while their counterparts filled with hollow nanoparticles have a much lower ρ_{eff} of ~1,246 kg/m^3 , ~1,135 kg/m^3 , and ~1,109 kg/m^3 , respectively (see **Table 2**). More interestingly, the effective mass density of the polymer nanocomposites filled with hollow Al, hollow Al_2O_3 , hollow AlN, and hollow BN even decreases with

the volume fraction of the nanoparticles. More specifically, the effective mass density of the polymer nanocomposites can be reduced from $\sim 1,000 \text{ kg/m}^3$ to $\sim 681 \text{ kg/m}^3$, $\sim 756 \text{ kg/m}^3$, $\sim 731 \text{ kg/m}^3$, and ~ 663

kg/m^3 when it is respectively filled with hollow Al, hollow Al_2O_3 , hollow AlN, and hollow BN nanoparticles at a V_f of 50 percent (see **Table 2**).

Table 2. Effect thermal conductivity and mass density for polymer nanocomposites filled with various solid, hollow, and graphene-wrapped hollow nanoparticles at a volume fraction of 50%.

Nanoparticle	$V_f = 50\%$	Ag	Al	Fe	Cu	Al_2O_3	AlN	BN
Solid	$\kappa_{\text{eff}} (\text{Wm}^{-1}\cdot\text{K}^{-1})$	28	14	3.6	20	4.1	22	5.0
	$\rho_{\text{eff}} (\text{kg/m}^3)$	5,646	1,849	4,374	4,971	2,380	2,097	1,663
Hollow	$\kappa_{\text{eff}} (\text{Wm}^{-1}\cdot\text{K}^{-1})$	1.9	1.2	0.5	1.7	0.5	1.4	0.6
	$\rho_{\text{eff}} (\text{kg/m}^3)$	1,246	681	1,109	1,135	756	731	663
Graphene-wrapped	$\kappa_{\text{eff}} (\text{Wm}^{-1}\cdot\text{K}^{-1})$	~ 11	~ 11	~ 5	~ 11	~ 5	~ 11	~ 5
	$\rho_{\text{eff}} (\text{kg/m}^3)$	1,290	817	1,153	1,196	877	847	789

Figure 2a shows the mapping result of the κ_{eff} as function of the thermal conductivity of the filler material (κ_{filler}) and V_f for the polymer nanocomposites filled with hollow nanoparticles. The calculations in **Figure 1e** are included in this more comprehensive mapping result. For example, for nanocomposites filled with 10 vol.% hollow AlN, 20 vol.% hollow Cu, 30 vol.% hollow Al, and 40 vol.% hollow Ag nanoparticles, which are marked on **Figure 2e**, they have a κ_{eff} of $\sim 0.31 \text{ Wm}^{-1}\cdot\text{K}^{-1}$, $\sim 0.41 \text{ Wm}^{-1}\cdot\text{K}^{-1}$, $\sim 0.54 \text{ Wm}^{-1}\cdot\text{K}^{-1}$, $\sim 0.91 \text{ Wm}^{-1}\cdot\text{K}^{-1}$, respectively, as indicated by the color bar. The κ_{eff} increases with both κ_{filler} and V_f . At $\kappa_{\text{filler}} = 2000 \text{ Wm}^{-1}\cdot\text{K}^{-1}$ and $V_f = 50\%$, the effective thermal conductivity can be increased to $\sim 4.8 \text{ Wm}^{-1}\cdot\text{K}^{-1}$. In contrast, **Figure 2b** shows the mapping result for the nanocomposite filled with solid nanoparticles. The solid nanoparticles are indeed more effective in enhancing the κ_{eff} than their hollow

counterparts. For example, at $\kappa_{\text{filler}} = 2000 \text{ Wm}^{-1}\cdot\text{K}^{-1}$ and $V_f = 50\%$, the κ_{eff} can be enhanced to $\sim 103 \text{ Wm}^{-1}\cdot\text{K}^{-1}$ by the solid nanoparticles.

However, in order to achieve a specific thermal conductivity by filling different types of nanoparticles into the PE polymer, the nanocomposites filled with hollow nanoparticles are shown to require much less filler materials and hence show much lower mass density. For example, as shown in **Figure 3a**, for a PE nanocomposite with an effective thermal conductivity of $\sim 1 \text{ Wm}^{-1}\cdot\text{K}^{-1}$, the mass density is $\sim 3,566 \text{ kg/m}^3$, $\sim 1,506 \text{ kg/m}^3$, $\sim 3,206 \text{ kg/m}^3$, and $\sim 1,614 \text{ kg/m}^3$ when the nanocomposite is filled with solid Ag, solid Al, solid Cu, and solid AlN nanoparticles, respectively. However, their counterparts only show a mass density of $\sim 1,271 \text{ kg/m}^3$, $\sim 774 \text{ kg/m}^3$, $\sim 1,156 \text{ kg/m}^3$, and $\sim 805 \text{ kg/m}^3$ when filled with the corresponding hollow nanoparticles.

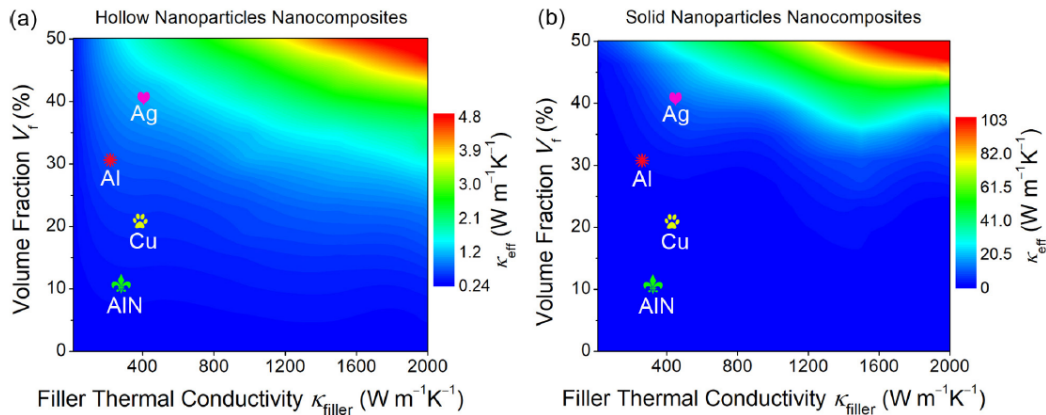


Figure 2. The effective thermal conductivity as function of the volume fraction and the filler thermal conductivity for polymer nanocomposites filled with (a) hollow nanoparticles and (b) solid nanoparticles.

Furthermore, the materials cost in the nanocomposites filled with the hollow nanoparticles will also be much less. As shown in **Figure 3b**, the unit costs of the polymer nanocomposites filled with hollow Ag, hollow Al, hollow Cu, and hollow AlN nanoparticles are ~ 0.839 $\$/\text{cm}^3$, ~ 0.001 $\$/\text{cm}^3$, ~ 0.0069 $\$/\text{cm}^3$, and ~ 0.161 $\$/\text{cm}^3$, while the unit costs of their counterparts filled with solid nanoparticles are ~ 2.35 $\$/\text{cm}^3$, ~ 0.0019 $\$/\text{cm}^3$, ~ 0.019 $\$/\text{cm}^3$, and ~ 0.322 $\$/\text{cm}^3$, respectively. Therefore, the usage of hollow nanoparticles reduces the weight of the nanocomposite and the materials cost of the nanocomposite. However, the hollow nanoparticles might not yield sufficient enhancement of the effective thermal conductivity. For instance, by filling hollow nanoparticles such as Fe, Al_2O_3 , and BN into the PE polymer, a target κ_{eff} of $1 \text{ Wm}^{-1}\cdot\text{K}^{-1}$ may not be achieved unless denser PE polymer with higher thermal conductivity is used as the matrix.

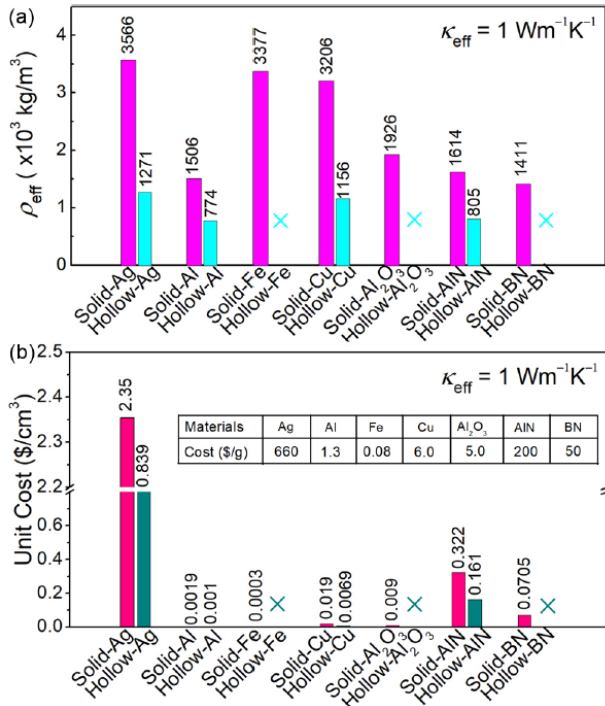


Figure 3. For a PE nanocomposite with a targeted effective thermal conductivity of 1 WKlml , (a) the mass density and (b) the unit cost of materials it has when it is filled with various solid and hollow nanoparticles. The inset Table of (b) lists the rough costs of different filler materials, which might change depending on the market.

In the light of the mapping result for the κ_{eff} as function of the κ_{filler} and the V_f shown in **Figure 2a**, we propose a hierarchical architecture for

the hollow nanoparticles. As shown in **Figure 4**, we suggest wrapping one graphene layer onto the shell of the hollow nanoparticle. This design is rationalized by the super-high thermal conductivity ($\sim 4,000 \text{ Wm}^{-1}\cdot\text{K}^{-1}$) of the graphene^[41,42], which can be employed to possibly wrap the shell of a hollow nanoparticle^[43-45]. The technique of wrapping a graphene layer onto the shell of a nanoparticle has been used to improve the performances of batteries^[43-45], and here we predict that it can be used to improve the effective thermal conductivity of the polymer nanocomposites.

It can be seen from **Figure 5a** that the effective thermal conductivity of the nanocomposite filled with graphene-wrapped hollow nanoparticles increases much faster with the volume fraction of the filler nanoparticles. At a V_f of 50%, the effective thermal conductivity of the nanocomposite can be enhanced to $\sim 11 \text{ Wm}^{-1}\cdot\text{K}^{-1}$, which is about 10 times of their counterparts filled with hollow nanoparticles without a graphene layer. Meanwhile, this hierarchical architecture does not increase the effective mass density much. As shown in **Figure 5b**, the effective mass density of the nanocomposite at a V_f of 50% is $\sim 1,290 \text{ kg/m}^3$, $\sim 817 \text{ kg/m}^3$, $\sim 1,153 \text{ kg/m}^3$, $\sim 1,196 \text{ kg/m}^3$, $\sim 877 \text{ kg/m}^3$, $\sim 847 \text{ kg/m}^3$, and $\sim 789 \text{ kg/m}^3$ when filled with graphene-wrapped hollow Ag, Al, Fe, Cu, Al_2O_3 , AlN, and BN nanoparticles, respectively (see **Table 2**). These values are about $\sim 3.5\%$, $\sim 20.0\%$, $\sim 3.9\%$, $\sim 5.3\%$, $\sim 16.0\%$, $\sim 15.8\%$, and $\sim 19.0\%$ higher than their counterparts filled with corresponding hollow nanoparticles without wrapping graphene.

Figure 6a shows the comparison of the effective mass density between the nanocomposites filled with solid nanoparticles and graphene-wrapped hollow nanoparticles. It can be seen that a target κ_{eff} of $1 \text{ Wm}^{-1}\cdot\text{K}^{-1}$ now can be achieved by all listed filler materials. The effective mass densities of the nanocomposites filled with graphene-wrapped hollow nanoparticles are much lower than their counterparts filled with solid nanoparticles. For nanocomposites filled with heavy fillers such as Ag, Fe, and Cu, the effective mass density can be reduced by $\sim 70\%$ by using graphene-wrapped hollow nanoparticles rather than solid nanoparticles, while still preserving the

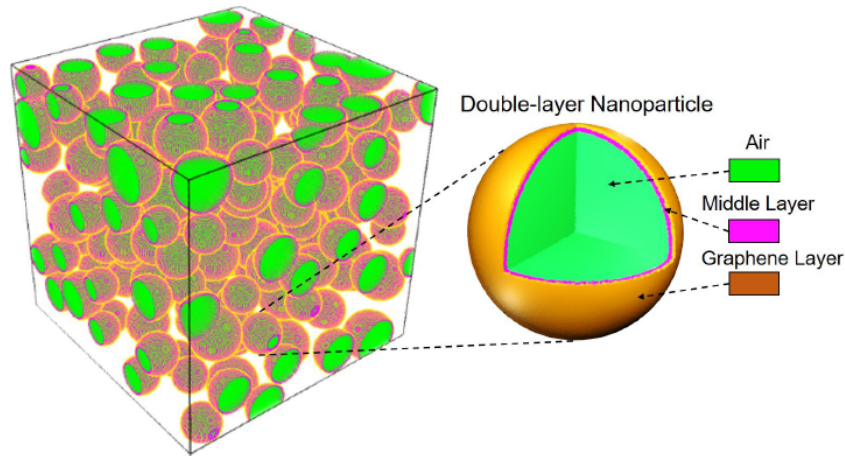


Figure 4. The microstructure of a polymer nanocomposite filled with a double-layer nanoparticle where the outer layer is graphene.

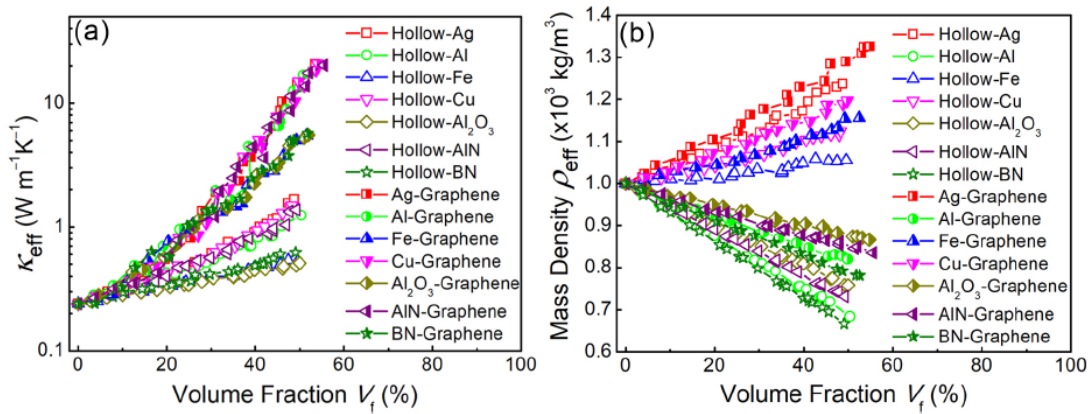


Figure 5. (a) The effective thermal conductivity and (b) mass density as function of filler volume fraction for polymer nanocomposites filled with graphene-wrapped hollow nanoparticles, compared with their counterparts without graphene layer.

same κ_{eff} of $1 \text{ W m}^{-1} \cdot \text{K}^{-1}$. This is not only beneficial to the reduction of the weight and materials costs, but also beneficial to the preservation of the flexibility performances of the polymers which can easily be damaged by a high loading level^[46–50]. As shown in **Figure 6b**, the V_f of the nanocomposites filled with graphene-wrapped hollow nanoparticles is universally reduced, compared with the counterpart in the nanocomposites filled with solid nanoparticles.

Now turn to the underlying mechanisms of the advantages of using hollow nanoparticles and graphene-wrapped nanoparticles over the solid nanoparticles. We consider three nanocomposites, which are filled with solid nanoparticles, hollow nanoparticles, and graphene-wrapped hollow nanoparticles, respectively. The filler materials are same, e.g., Cu metal, and the sizes of the filler nanoparticles are assumed to be similar. The volume fraction of Cu metal in the three nanocomposites

are set to be at the same value of 6%. While in the nanocomposite filled with solid nanoparticles the thermally conductive Cu metal concentrates at each solid particle, the Cu metal in the nanocomposite filled with hollow nanoparticles distributes on the surface of each hollow particle. Since the surface layer volume of the hollow particle is much lower than the whole volume of the solid particle, there must be more hollow particles in the same polymer. As a result, the probability of forming thermally conductive channels through surfaces connection of the hollow particles is increased, leading to the enhancement of the effective thermal conductivity. This can be understood from the comparison of the thermal energy flux distributions shown in **Figures 7a-b**. By wrapping a more thermally conductive graphene layer on the surfaces of the hollow nanoparticles, the formation probability of heat conductive channels and hence the effective thermal conductivity will be

further increased, as revealed in **Figure 7c**.

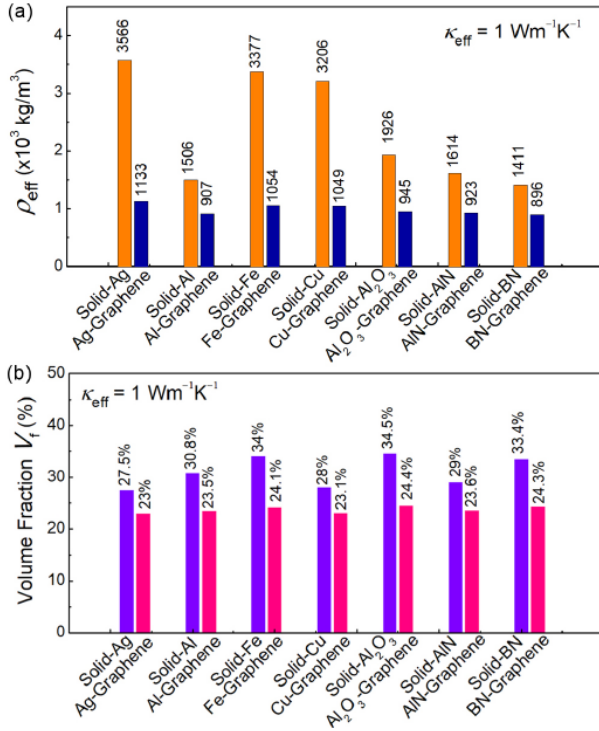


Figure 6. For a PE nanocomposite with a targeted effective thermal conductivity of 1 WKlml, **(a)** the mass density and **(b)** the filler volume fraction it has when it is filled with various solid and graphene-wrapped hollow nanoparticles.

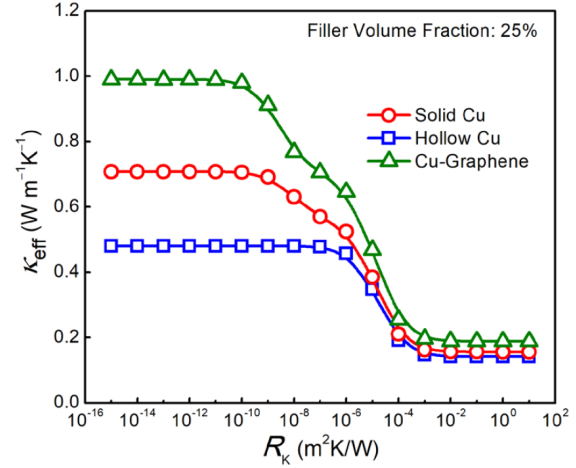


Figure 8. Effect of the interfacial thermal resistance on the effective thermal conductivity for PE nanocomposites filled with 25 vol.% solid Cu nanoparticles, hollow Cu nanoparticles, and graphene-wrapped hollow Cu nanoparticles.

In above simulations, the strategy of adding hollow and graphene-wrapped hollow nanoparticles into the polymer to enhance the thermal conductivity and reduce the mass density is illustrated without considering the interfacial thermal resistance (R_k). **Figure 8a** shows the parameterized study of R_k effects on the effective thermal conductivity for polymer nano-

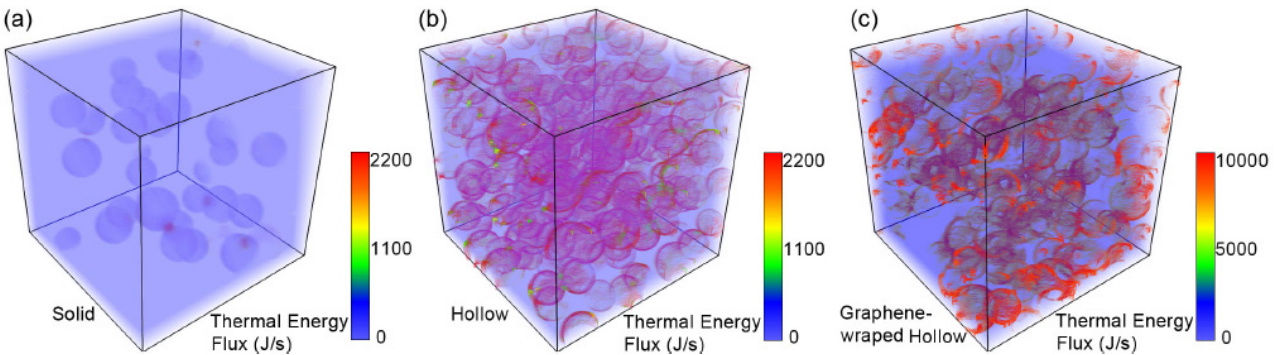


Figure 7. Thermal energy flux distributions for polymer nanocomposites filled with **(a)** solid Cu nanoparticles, **(b)** hollow Cu nanoparticles, and **(c)** graphene-wrapped hollow Cu nanoparticles. The volume fractions of Cu metal for these three polymer nanocomposites are at the same value of 6%. Due to the introduction of the hollow structure, the volume fractions of the hollow nanoparticles are 30%.

composites filled with solid, hollow, and graphene-wrapped Cu hollow nanoparticles. For polymer nanocomposites filled with solid Cu and graphene-wrapped hollow Cu nanoparticles, R_k is important when it is greater than $10^{-10} \text{ m}^2\text{K/W}$, whereas it is important when $R_k > 10^{-6} \text{ m}^2\text{K/W}$ for the polymer nanocomposite filled with hollow Cu nanoparticles. Specifically, the effective thermal conductivity can be

decreased by the interfacial thermal resistance from $1.0 \text{ Wm}^{-1}\text{K}^{-1}$ to $0.19 \text{ Wm}^{-1}\text{K}^{-1}$, from $0.71 \text{ Wm}^{-1}\text{K}^{-1}$ to $0.16 \text{ Wm}^{-1}\text{K}^{-1}$, and from $0.48 \text{ Wm}^{-1}\text{K}^{-1}$ to $0.14 \text{ Wm}^{-1}\text{K}^{-1}$ for polymer nanocomposite filled with 25 vol.% graphene-wrapped hollow Cu nanoparticles, solid Cu nanoparticles, and hollow Cu nanoparticles, respectively. Therefore, the effective thermal conductivity predicted in this work should be lower

when the interfacial thermal resistance is considered. In order to accurately predict the effective thermal conductivity as function of the microstructure, the knowledge of the interfacial thermal resistance is necessary. While it is challenging to measure the interfacial thermal resistance experimentally, it may be obtained via molecular dynamic simulations^[51–53].

3. Conclusions

The effective thermal conductivity and effective mass density of the polymer nanocomposites filled with solid nanoparticles and hollow nanoparticles are computed. It is predicted that the usage of hollow nanoparticles rather than the solid nanoparticles as fillers can enhance the thermal conductivity but preserve the low mass density of the polymer nanocomposites. By wrapping a graphene layer onto the surface of the hollow nanoparticles, the effective thermal conductivity can be further significantly enhanced while still preserving a low mass density of the polymer nanocomposite. The underlying mechanism of this microstructure design and the quantitative effect of the interfacial thermal resistance are presented. The present work is expected to stimulate future experimental and theoretical efforts to design light-weight thermally conductive polymer nanocomposites.

Conflict of interest

No conflict of interest was reported by the authors.

Acknowledgements

J. J. Wang and L. Q. Chen are partially supported by the US Air Force Office of Scientific Research through tasks (FA9550-17-1-0318) and by the Hamer Professorship. W Y Zhou gratefully acknowledge the financial supports from the National Natural Science Foundation of China (No.51577154), the Key Laboratory of Engineering Dielectrics and Its Application, Ministry of Education, Harbin University of Science and Technology (No. JZK201301, KF20151111).

References

1. Gurrum SP, Suman SK, Joshi YK, *et al.* Thermal issues in next-generation integrated circuits. *IEEE Transactions on Device and Materials Reliability* 2004; 4 (4): 709–714.
2. Ghosh S, Calizo I, Teweldebrhan D, *et al.* Extremely high thermal conductivity of graphene: Prospects for thermal management applications in nanoelectronic circuits. *Applied Physics Letters* 2008; 92 (15): 151911.
3. Otiaba KC, Ekere NN, Bhatti R, *et al.* Thermal interface materials for automotive electronic control unit: trends, technology and R&D challenges. *Microelectronics Reliability* 2011; 51(12): 2031–2043.
4. Moore AL, Shi L. Emerging challenges and materials for thermal management of electronics. *Materials Today* 2014; 17(4): 163–174.
5. Chen H, Ginzburg VV, Yang J, *et al.* Thermal conductivity of polymer-based composites: Fundamentals and applications. *Progress in Polymer Science* 2016; 59: 41–85.
6. Tong X. *Advanced materials for thermal management of electronic packaging*. New York: Springer Science & Business Media; 2011.
7. Han Z, Fina A. Thermal conductivity of carbon nanotubes and their polymer nanocomposites: A review. *Progress in polymer science* 2011; 36(7): 914–944.
8. T'Joen C, Park Y, Wang Q, *et al.* A review on polymer heat exchangers for HVAC&R applications. *International Journal of Refrigeration* 2009; 32(5): 763–779.
9. Gojny FH, Wichmann MH, Fiedler B, *et al.* Evaluation and identification of electrical and thermal conduction mechanisms in carbon nanotube/epoxy composites. *Polymer* 2006; 47(6): 2036–2045.
10. Marconnet AM, Yamamoto N, Panzer MA, *et al.* Thermal conduction in aligned carbon nanotube—Polymer nanocomposites with high packing density. *ACS Nano* 2011; 5(6): 4818–4825.
11. Rahmat M, Hubert P. Carbon nanotube—Polymer interactions in nanocomposites: A preview. *Composites Science and Technology* 2011; 72(1): 72–84.
12. Du Y, Shen SZ, Cai K, *et al.* Research progress on

- polymer–inorganic thermoelectric nanocomposite materials. *Progress in Polymer Science* 2012; 37(6): 820–841.
13. Liu Y, Kumar S. Polymer/carbon nanotube nano composite fibers—A review. *ACS Applied Materials & Interfaces* 2014; 6(9): 6069–6087.
 14. Das TK, Prusty S. Graphene-based polymer composites and their applications. *Polymer-Plastics Technology and Engineering* 2013; 52(4): 319–331.
 15. Potts JR, Dreyer DR, Bielawski CW, *et al.* Graphene-based polymer nanocomposites. *Polymer* 2011; 52(1): 5–25.
 16. Shahil KM, Balandin AA. Graphene–multilayer graphene nanocomposites as highly efficient thermal interface materials. *Nano Letters* 2012; 12(2): 861–867.
 17. Li B, Zhong WH. Review on polymer/graphite nanoplatelet nanocomposites. *Journal of materials science* 2011; 46(17): 5595–5614.
 18. Wang M, Hu N, Zhou L, *et al.* Enhanced interfacial thermal transport across graphene–polymer interfaces by grafting polymer chains. *Carbon* 2015; 85: 414–421.
 19. Zhou W, Qi S, Tu C, *et al.* Effect of the particle size of Al₂O₃ on the properties of filled heat-conductive silicone rubber. *Journal of Applied Polymer Science* 2007; 104(2): 1312–1318.
 20. Moreira D, Sphaier L, Reis J, *et al.* Experimental investigation of heat conduction in polyester–Al₂O₃ and polyester–CuO nanocomposites. *Experimental Thermal and Fluid Science* 2011; 35(7): 1458–1462.
 21. Zhang S, Cao X, Ma Y, *et al.* The effects of particle size and content on the thermal conductivity and mechanical properties of Al₂O₃/high density polyethylene (HDPE) composites. *Express Polymer Letters* 2011; 5(7): 581–590.
 22. Zhi C, Bando Y, Tang C, *et al.* Large-scale fabrication of boron nitride nanosheets and their utilization in polymeric composites with improved thermal and mechanical properties. *Advanced Materials* 2009; 21(28): 2889–2893.
 23. Huang X, Zhi C, Jiang P, *et al.* Polyhedral oligosilsesquioxane-modified boron nitride nanotube based epoxy nanocomposites: an ideal dielectric material with high thermal conductivity. *Advanced Functional Materials* 2013; 23(14): 1824–1831.
 24. Song WL, Wang P, Cao L, *et al.* Polymer/boron nitride nanocomposite materials for superior thermal transport performance. *Angewandte Chemie International Edition* 2012; 51(26): 6498–6501.
 25. Li TL, Hsu SLC. Preparation and properties of thermally conductive photosensitive polyimide/boron nitride nanocomposites. *Journal of Applied Polymer Science* 2011; 121(2): 916–922.
 26. Li Q, Chen L, Gadinski MR, *et al.* Flexible high-temperature dielectric materials from polymer nanocomposites. *Nature* 2015; 523(7562): 576.
 27. Mamunya YP, Davydenko V, Pissis P, *et al.* Electrical and thermal conductivity of polymers filled with metal powders. *European Polymer Journal* 2002; 38(9): 1887–1897.
 28. Chung D. Materials for thermal conduction. *Applied Thermal Engineering* 2001; 21(16): 1593–1605.
 29. Wang S, Cheng Y, Wang R, *et al.* Highly thermal conductive copper nanowire composites with ultralow loading: toward applications as thermal interface materials. *ACS Applied Materials & Interfaces* 2014; 6(9): 6481–6486.
 30. Bjorneklett A, Halbo L, Kristiansen H. Thermal conductivity of epoxy adhesives filled with silver particles. *International Journal of Adhesion and Adhesives* 1992; 12(2): 99–104.
 31. Pashayi K, Fard HR, Lai F, *et al.* High thermal conductivity epoxy-silver composites based on self-constructed nanostructured metallic networks. *Journal of Applied Physics* 2012; 111(10): 104310.
 32. Burger N, Laachachi A, Ferriol M, *et al.* Review of thermal conductivity in composites: Mechanisms, parameters and theory. *Progress in Polymer Science* 2016; 61: 1–28.
 33. King JA, Tucker KW, Vogt BD, *et al.* Electrically and thermally conductive nylon 6, 6. *Polymer Composites* 1999; 20(5): 643–654.
 34. Fan L, Khodadadi JM. Thermal conductivity enhancement of phase change materials for thermal energy storage: A review. *Renewable and Sustainable Energy Reviews* 2011; 15(1): 24–46.
 35. Wang JJ, Wang Y, Ihlefeld JF, *et al.* Tunable thermal conductivity via domain structure engineering in ferroelectric thin films: A phase-field simulation. *Acta*

- Materialia 2016; 111: 220–231.
36. Wang J, Ma X, Li Q, *et al.* Phase transitions and domain structures of ferroelectric nanoparticles: Phase field model incorporating strong elastic and dielectric inhomogeneity. *Acta Materialia* 2013; 61(20): 7591–7603.
 37. Wang J, Song Y, Ma X, *et al.* Static magnetic solution in magnetic composites with arbitrary susceptibility inhomogeneity and anisotropy. *Journal of Applied Physics* 2015; 117(4): 043907.
 38. Parker W, Jenkins R, Butler C, *et al.* Flash method of determining thermal diffusivity, heat capacity, and thermal conductivity. *Journal of Applied Physics* 1961; 32(9): 1679–1684.
 39. Lee W, Han I, Yu J, *et al.* Thermal characterization of thermally conductive underfill for a flip-chip package using novel temperature sensing technique. *Thermo-chimica Acta* 2007; 455(1-2): 148–155.
 40. Zhou W, Qi S, An Q, *et al.* Thermal conductivity of boron nitride reinforced polyethylene composites. *Materials Research Bulletin* 2007; 42(10): 1863–1873.
 41. Stankovich S, Dikin DA, Dommett GHA, *et al.* Graphene-based composite materials. *Nature* 2006; 442(7100): 282.
 42. Kim SY, Noh YJ, Yu J. Thermal conductivity of graphene nanoplatelets filled composites fabricated by solvent-free processing for the excellent filler dispersion and a theoretical approach for the composites containing the geometrized fillers. *Composites Part A: Applied Science and Manufacturing* 2015; 69: 219–225.
 43. Tu W, Zhou Y, Liu Q, *et al.* Robust hollow spheres consisting of alternating titania nanosheets and graphene nanosheets with high photocatalytic activity for CO₂ conversion into renewable fuels. *Advanced Functional Materials* 2012; 22(6): 1215–1221.
 44. Wang H, Yang Y, Liang Y, *et al.* Graphene-wrapped sulfur particles as a rechargeable lithium–sulfur battery cathode material with high capacity and cycling stability. *Nano Letters* 2011; 11(7): 2644–2647.
 45. Wu P, Wang H, Tang Y, *et al.* Three-dimensional interconnected network of graphene-wrapped porous silicon spheres: In situ magnesiothermic-reduction synthesis and enhanced lithium-storage capabilities. *ACS Applied Materials & Interfaces* 2014; 6(5): 3546–3552.
 46. Dasari A, Yu ZZ, Mai YW. Fundamental aspects and recent progress on wear/scratch damage in polymer nanocomposites. *Materials Science and Engineering: R: Reports* 2009; 63(2): 31–80.
 47. Li F, Hu K, Li J, *et al.* The friction and wear characteristics of nanometer ZnO filled polytetrafluoroethylene. *Wear* 2001; 249(10–11): 877–882.
 48. Ding H, Guo Y, Leung SN. Development of thermally conductive polymer matrix composites by foaming-assisted networking of micron-and submicron-scale hexagonal boron nitride. *Journal of Applied Polymer Science* 2016; 133(4): 42910.
 49. Woltornist SJ, Varghese D, Massucci D, *et al.* Controlled 3D assembly of graphene sheets to build conductive, chemically selective and shape-responsive materials. *Advanced Materials* 2017; 29(18): 1604947.
 50. Okamoto M, Nam PH, Maiti P, *et al.* Biaxial flow-induced alignment of silicate layers in polypropylene/clay nanocomposite foam. *Nano Letters* 2001; 1(9): 503–505.
 51. Zhong H, Lukes JR. Interfacial thermal resistance between carbon nanotubes: Molecular dynamics simulations and analytical thermal modeling. *Physical Review B* 2006; 74(12): 125403.
 52. Diao J, Srivastava D, Menon M. Molecular dynamics simulations of carbon nanotube/silicon interfacial thermal conductance. *The Journal of Chemical Physics* 2008; 128(16): 164708.
 53. Stevens RJ, Zhigilei LV, Norris PM. Effects of temperature and disorder on thermal boundary conductance at solid–solid interfaces: Nonequilibrium molecular dynamics simulations. *International Journal of Heat and Mass Transfer* 2007; 50(19, 20): 3977–3989.